핵자기 공명 영상 에서 새로운 유속 흐름제거 방법

노용만, 조장희
한국과학기술원 전기및 전자 공학과

Novel Flow Suppression Technique in MRI

Y. M. Ro and Z. H. Cho
Dept. of Electrical Science, Korea Advanced Institute of Science and Technology, P.O. Box 150, Chongyangni, Seoul, Korea

ABSTRACT

The pulsatile nature of blood flow makes artefacts in 2D Fourier transform image. Spatial presaturation is known to be effective in eliminating flow artefacts when the spin echo acquisition is employed. However, this method requires additional RF pulse and spoiling gradient for presaturation. In this paper a new flow saturation technique which does not require additional saturation-RF and gradient is proposed. The proposed technique is equivalent to the existing saturation technique but the elimination of the flow component is achieved by a pair of tailored 90°-180° RF pulses in the spin echo sequence. By use of two tailored RF pulses with opposite phase polarity, a linear phase gradient is generated for those moving materials and consequently all the spins of moving materials become dephased thereby no signal is observable. Computer simulations and experimental results obtained using both a phantom and a human volunteer with a 2.0 T whole body system are also presented.

I. INTRODUCTION

In the conventional Fourier NMR imaging, image blurs of non-moving tissues as well as blood itself are observed due to the flow effects of blood (1-3). This is due to modulation effect of the flow phenomena on the magnitude as well as phase of the magnetization within a voxel in NMR imaging (4,5). As is known, the varying flow velocity which is due to the pulsatile blood flow related with pumping of heart makes the distribution of the magnitudes and phases of signal random thereby produces zipper-like artefacts in the direction to the phase encoding in 2D Fourier transform imaging.

To reduce this flow artefact, several techniques have been developed such as the ECG gating, spatial presaturation, cardiac cycle reordered phase encoding technique and gradient moment nulling etc. (6-10). In the cardiac cycle reordered phase encoding technique and gradient moment nulling, the flow artefacts are reduced by synchronizing the pulsatile phase fluctuation during the imaging time. Same is true also in ECG gated imaging where data acquisition is synchronized with ECG signals and thereby reduces flow artefacts. In the presaturation technique, the reduction of flow artefacts is achieved by saturating the inflow materials before actual imaging data acquisition takes place (11). This spatial presaturation of inflow to the imaging slice is achieved by 90° RF pulse with subsequent spoiling-gradients.

In this paper, two tailored RF pulses are used, for example 90° and 180° RF pulses with spin echo sequence. Each RF pulse has a quadratic phase distribution within a selected slice but with has opposite phase distribution (12,13). Consequently, in a voxel having flow, a linear phase gradient will be developed when they are combined (see Fig. 3 (c)). All the spins in the flow or moving materials, therefore, become incoherent or dephased simply due to the resultant linear phase gradient created within the voxel. For the spins in static material, however, will be different as a result of addition of two opposing quadratic phase distributions which will result a constant phase or zero phase gradient as shown in Fig. 3 (b).

II. THEORY AND METHODS

1. Flow Artefacts in 2D Fourier Transform Spin Echo Imaging

Flow Artefacts in 2D Fourier transform images obtained by spin echo imaging are generally produced by two reasons. First one is the signal magnitude fluctuation of intravoxel magnetization between the different encoding steps. The other is the phase fluctuation of intravoxel magnetization between different encoding steps. In spin echo imaging, the intravoxel signals of moving material excited by two RF pulses, i.e., 90° and 180° RF pulses are different in each encoding step due to its time-varying nature as shown in Fig. 1. In this case the overlapping area represents the signal amplitude, i.e., higher the velocity smaller the signal. Let us define the magnitude and phase of an intravoxel signal as $m(v_k)$ and $\phi(v_k)$ where v_k is a

velocity corresponding to k-th encoding step and all the spins within a selected voxel are assumed to have same magnitude and velocity.

First, let us consider magnitude fluctuation. This situation is illustrated in Fig. 1 and the magnitude of the intravoxel signal of moving material can be given by

$$m(v_k) = \int_{voxel} M dz$$

$$= M(z_o - \frac{T_E v_k}{2}), \quad [1]$$

where M is the magnitude of spin magnetization and z_0 is the slice thickness, and T_E is the echo time. Here it is assumed that the voxel sizes of transverse domain (i.e., x and y directions in this case) are relatively small compared with the thickness (z_0) and also normalized. The voxel signal is, therefore, only dependent on the z-direction or slice thickness and the integration of magnetization of selected slice (z-direction) as shown in Eq. [1]. It is, therefore, evident that the magnitude $m(v_k)$ of the flow would be different at different encoding steps for the time varying v_k.

The other fluctuating factor is the phase of the signal from the moving material, $\phi(v_k)$. Since the phase $\phi(v_k)$ is subject to fluctuation by the magnetic field gradients applied during the time interval between the RF excitation and data acquisition in conjunction with the flow velocity, v_k, i.e.,

$$\phi(v_k) = \gamma\, v_k \int_0^{T_E} \{G_z(t) + G_{sus}\} t\, dt, \quad [2]$$

where γ is the gyromagnetic ratio, $G_z(t)$ is the magnetic field gradient along z direction, and G_{sus} is the susceptibility dependent field gradient. As is seen from Eq. [2], phase of the intravoxel signal of a moving material is time varying due to the time varying v_k, i.e., each v_k gives different phase $\phi(v_k)$. Note here v_k is assumed constant during the time interval of each encoding step.

The total signal from a voxel at k-th encoding step can, therefore, be written as,

$$s(v_k) = m(v_k)\exp[i\phi(v_k)], \quad [3]$$

Consequently $s(v_k)$ fluctuates at each encoding step depending on the magnitude $m(v_k)$ and phase $\phi(v_k)$. As is known, in the Fourier transform imaging, the fluctuating signal produces image blur especially in the direction of the phase encoding. The extent of blur can be characterized in the direction of phase encoding as

$$\int s(v_k)\exp(i\omega_k k)dk, \quad [4]$$

where ω_k is the frequency variable of the phase encoding direction ($\omega_k = \gamma g_k T_k$, where g_k and T_k are the amplitude and pulse duration of the encoding gradient, respectively). An example of the blur function of a moving material with random fluctuation is shown in Fig. 2(a). As shown in Fig. 2(a), the point spread function is completely dispersed in the coding direction and this is translated in the reconstructed image as an image blur. An example of this type of blur is the blood flow. For a simple comparison, a blur function due to the non-flow sample or the static material is shown in Fig. 2(b). The latter, in an ideal situation, would show a delta function like point spread function (PSF) as it should.

2. Flow suppression using tailored RF pulses in Spin Echo Sequence

Let us now study how those blur functions can be eliminated by use of a set of tailored RF pulses, i.e., tailored 90° and 180° RF pulses. As mentioned above, flowing material makes an artefact due to its time varying nature. In order to reduce or eliminate the flow artefact, the phase of the fluctuating flow should be made constant for all the encoding steps (such as gradient moment nulling or ECG gating method) or saturate the flow component before entering into the imaging slice so that no observable signal (such as presaturation method) is produced during the imaging sequence (11).

In normal 90°-180° spin echo imaging sequence, flow component excited by 90° pulse is moved forward along the direction of flow until the arrival of the 180° pulse, i.e., half of the echo time or the time interval between 90° and 180° RF pulses. Since the signal magnitude of the flow component is dependent on the flow velocity as shown in Fig. 1, the flow signals would differ in magnitudes and phases at different phase encoding steps. Now, if a set of tailored RF pulses, i.e., 90° and 180° RF pulses each of which has a quadratic phase of different polarity (see Fig. 3 (a)) is applied on a static material, the combined phase distribution generated within a selected slice would be a constant phase within a voxel since each phase distribution cancels out the other, i.e., first 90° pulse with positive phase distribution would cancel out the following 180° pulse which has negative phase distribution as shown in Fig. 3 (b) (12). On the other hand, same set of pulses are applied on the flowing materials, situation would be different and will create linear phase gradient as shown in Fig. 3 (c). Therefore, by use of a set of appropriate tailored RF pulses, it is possible to create any desired phase distributions with in a voxel for both the static and moving materials. Another word, in the case of static material, the quadratic phase generated by 90° RF pulse is canceled out by an opposite polarity-quadratic phase generated by 180° RF pulse and thereby becomes constant phase distribution as shown in Fig. 3 (b). The signal intensity of static voxel, therefore, is not affected. On the other hand, when a same set of pulses

(quadratic phase) is applied on a moving material, a linear phase gradient will be created as shown in Fig. 3 (c) and consequently the signal strength resulting from the linear phase distribution reduces the signal intensity. This, indeed, is unique and useful aspects of the method and can be applicable to many areas of flow measurements as well as flow artefact suppression as will be detailed in the following.

Let a flowing material is excited by a set of tailored 90° and 180° RF pulses, signal due to the spins in an infinitesimally small intravoxel at k-th encoding step can be written as

$$\begin{aligned} ds(v_k) &= M\exp[i\phi(v_k)]\exp[i(\phi_{90^\circ} - \phi_{180^\circ})] \\ &= M\exp[i\phi(v_k)]\exp[i\{\alpha(z-d)^2 - \alpha z^2\}] \\ &= M\exp[i\phi(v_k)]\exp[-i\alpha d(2z-d)], \end{aligned} \quad [5]$$

where $\phi_{90^\circ} = \alpha(z-d)^2$, $\phi_{180^\circ} = -\alpha z^2$, α is a constant and d is the distance moved by the flow during the time interval between 90° and 180° RF pulses, i.e., $\frac{v_k T_E}{2}$ as shown in Fig. 1. In Eq. [5], it is shown that a linear phase gradient or phase distribution along the slice selection direction (z-direction) will always be created when two tailored RF pulses are added, i.e., 90° and 180° pulses (see Fig. 3 (c)). The signal intensity of the voxel containing moving material is also affected by the speed of flowing material and can be given as

$$s(v_k) = \int_d^{z_o} M\exp[i\phi(v_k)]\exp[-i\alpha d(2z-d)]dz. \quad [6]$$

Equation [6], as it should, would become simple integration along z when $d = 0$ or no flowing material, i.e., $s(v_k) = \int_0^{z_o} M\exp[i\phi(v_k)]dz$. The linear phase is, therefore, always generated by quadratic phases of two 90°and 180° tailored RF pulses thereby dephases all the spins of flowing material fairly independent to the flow velocity, v_k. Figure 4 shows the effect of the flow suppression as a function of flow velocity for several different quadratic phase coefficients α. As is shown, signal intensity due to flow is well suppressed for the wide range of velocity as long as quadratic phase coefficient value is large, i.e., $\alpha \geq 100$.

III. COMPUTER SIMULATIONS AND EXPERIMENTAL RESULTS

To verify the usefulness of the method, a series of computer simulations were performed. The phantom used for the simulation is shown in Fig. 5 (a). Two small circles represent the flowing materials and are located within the large cylinder filled with a static material. In addition the upper tube represents the flow with fluctuating velocity similar to pulsatile flow while the lower one is made of a constant velocity flow. In simulation, the thickness of phantom was assumed 10 mm, and the echo time was set to 40 msec. The velocity of the pulsatile flow of the upper tube was varied from 0 to 50 cm/sec while the lower tube was kept a constant velocity of 20 cm/sec.

In the conventional 90°-180° spin echo sequence, as expected, the pulsatile flow of upper tube makes the image blurred as shown in Fig. 5 (b) while, in the lower tube having a constant flow velocity, no image blur was observed but with small reduction in signal intensity which decreases proportionately with the flow velocity, therefore, the flow distance during the time interval between 90° and 180° RF excitation. When the proposed flow compensation is used, the flow artefact of pulsatile flow is reduced as shown in Fig. 5 (c) and together with reduction in signal intensity by the linear phase gradient which dephases the spins in the voxel. Like the upper tube, in the lower tube where the flow velocity is constant, the signal intensity has also reduced by the linear phase gradient. This is in agreement with the theory we have developed, i.e., the overlapped quadratic phases generated by a set of 90° and 180° RF pulses produce a linear phase gradient which then dephases all the spins in the selected slice thereby leads to no observable signal intensity.

To verify the proposed method experimentally, an human imaging was performed with a 2.0 T whole body NMR system. Two legs of a human volunteer was imaged with spin echo imaging sequence. Slice thickness of 10 mm was chosen with echo time and repetition time of 40 msec and 300 msec, respectively. Figure 6 (a) shows an image obtained by the conventional 90° and 180° RF pulses. As is seen, the time varying pulsatile flow of arteries produced visible flow artefacts or blur along the phase encoding direction. With the proposed tailored 90° and 180° RF pulses, the same slice imaging was performed and artefact free image was obtained as shown in Fig. 6(b).

In summary, a new flow suppression technique using tailored 90° and 180° RF pulses is proposed and computer simulation and experimental studies were performed. The results shows usefulness of the method in suppression of the flow artefact in a simple manner. Principle of the method is the suppression of the flow signal by use of a set of tailored 90° and 180° RF pulses of opposite polarity-phase distributions. Combination of those two then produces a linear phase gradient or phase distribution within a selected voxel and if flow velocity is above a certain velocity the phase distribution becomes sufficiently large so that no signal will be generated. The proposed method, therefore, does not require additional pulses such as the saturation RF and spoiling gradient usually needed in the conventional flow suppression imaging by use

of presaturation method. Although this method is applied to a simple flow artefact correction, principle of the method can be extended to many other areas of NMR imaging of similar cases where the susceptibility effect often obscures the image quality.

REFERENCES

1. L. E. Crooks, C. M. Mills and P. L. Davis et al, *Radiology* **144**, 843 (1982).
2. W. H. Perman, P. R. Moran, R. A. Moran and M. A. Bernstein, *J. Comput. Assit. Tomogr.* **10**, 473 (1986).
3. J. P. Felmlee and R. L. Ehman, *Radiology* **164**, 559 (1987).
4. P. R. Moran, *Magn. Reson. Imag.* **2**, 197 (1982).
5. Y. S. Kim, C. W. Mun, K. J. Jung and Z. H. Cho, *Magn. Reson. Med.* **4**, 289 (1987).
6. J. L. Duerk, P. M. Pattany, *Magn. Reson. Imag.* **7**, 251 (1989).
7. J. Fram, K. D. Merboldt, W. Hanicke and A. Hasse, *Magn. Reson. Med.* **14**, 293 (1990).
8. D. Matthaei and A. Hasse, *Magn. Reson. Med.* **4**, 302 (1987).
9. P. M. Pattany, J. J. Phillips, L. C. Chiu, J. D. Lipcamon, J. L. Duerk, J. M. McNally and S. N. Mohapatra, *J. Comput. Assit. Tomogr.* **11**, 369 (1987).
10. M. H. Cho, W. S. Kim and Z. H. Cho, *Magn. Reson. Imag.* **8**, 395 (1990).
11. R. L. Ehman and J. P. Felmlee, *Magn. Reson. Med.* **14**, 293 (1990).
12. Z. H. Cho and Y. M. Ro, *Magn. Reson. Med.* **23**, 193 (1992).
13. D. Kunz, *Magn. Reson. Med.* **3**, 377 (1986).
14. S. Conolly, D. Nishimura, and A. Marcovski, *J. Magn. Reson.* **78**, 440 (1988).
15. Y. M. Ro and Z. H. Cho, accepted in *Magn. Reson. Med.* (1992).

FIGURE CAPTIONS

Figure 1. The flow effect of a selected slice or voxel when a slice is excited by both 90° and 180° RF pulses (shaded region). d is moving distance of flow voxel, v_k is flow velocity, and T_E is the echo time, respectively. Echo signal (integration of shaded region), therefore, fluctuates according to the coding steps since the velocity v_k differs one coding step to another.

Figure 2. The image blur functions of flowing (a) and static (b) materials. As seen, the flow induces the flow artefact or horizontal blur in coding direction while in the static material blur is virtually non-existence.

Figure 3. (a) The phase distribution of static voxel when only one tailored RF pulse is applied, i.e., either 90° or 180° RF pulse. (b) The resulting phase distribution when a voxel is excited by a set of tailored 90 ° and 180° RF pulses which are in opposite in phase distributions. As seen, the static voxel is not affected by the tailored RF pulses. (c) In the flow voxel, the linear phase gradient or distributions is generated depending on the flow velocity. Although degree of linear phase is varied according to the flow velocity, spin dephasing remains same, i.e., no signal.

Figure 4. The suppression of flow signal intensity as a function of flow velocity and coefficient of the quadratic phase, α. Calculations are performed by assuming that the slice thickness is 10 mm with echo time of 30 msec.

Figure 5. A phantom simulation study. (a) The upper tube (circle) has a pulsatile flow with velocity range of 0~50 cm/sec while the lower tube (circle) has a constant flow of 20 cm/sec. Background is static material. (b) The reconstructed image obtained when the conventional 90° and 180° RF pulses are applied. As seen, the image blur is observed due to the pulsatile flow of the upper tube but lower tube remained no artefact (no signal). (c) The artefact free reconstructed image obtained when the tailored 90° and 180° RF pulses are applied. As seen, the blur is suppressed and furthermore flow signals of the pulsatile flow as well as the constant flow are disappeared.

Figure 6. (a) Human leg image when the conventional 90° and 180° RF pulses is applied. As seen, artery having pulsatile flow produces the flow artefact in coding direction. (b) The same image obtained by using the tailored 90° and 180° RF pulse sequence on the same conditions as (b). As seen, the flow artefact is completely suppressed thereby the blood lumen and surrounding tissues are more clearly visible.

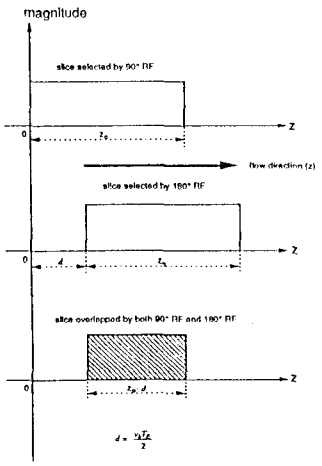

Figure 1

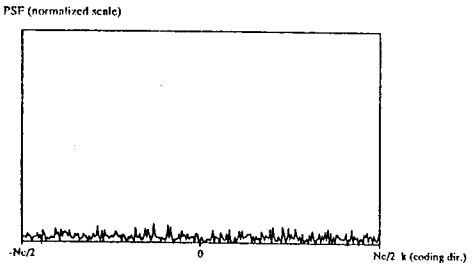

Image blur for the flowing material

Figure 2 (a)

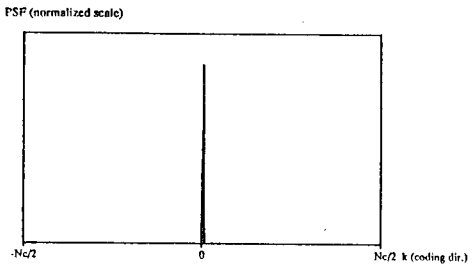

Image blur for the static material

Figure 2 (b)

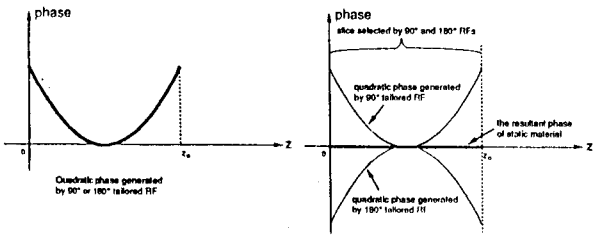

(a) (b)

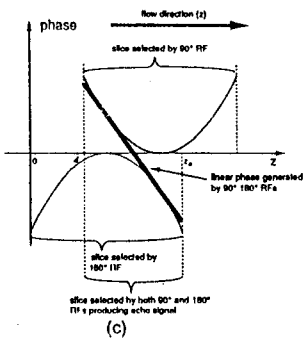

(c)

Figure 3

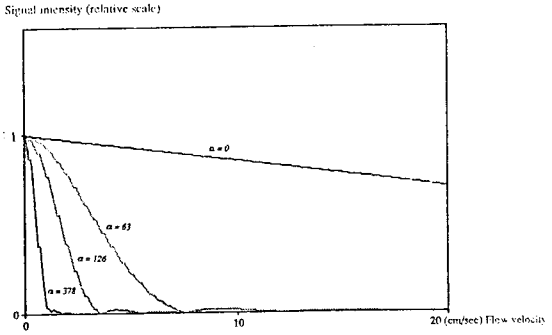

Figure 4

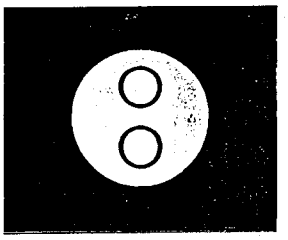

(a)

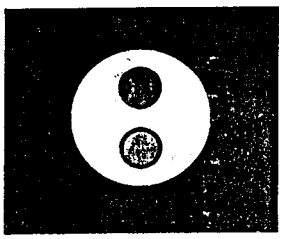

(b)

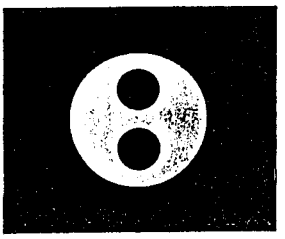

(c)

Figure 5

(a)

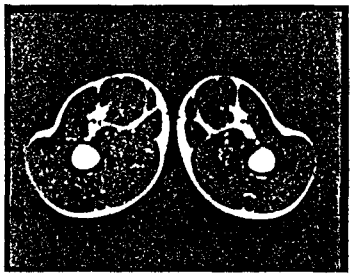

(b)

Figure 6